International Journal of Automotive Technology, Vol. 7, No. 3, pp. 251–259 (2006)

1229–9138/2006/027–03

INFLUENCE OF THE MIXING RATIO OF DOUBLE COMPONENTIAL FUELS ON HCCI COMBUSTION

S. SATO[1)*], S. P. KWEON[2)], D. YAMASHITA[2)] and N. IIDA[3)]

[1)]Environment Research Department, National Traffic Safety and Environment Laboratory, 7-42-27 Jindaiji-higashimachi, Chofu, Tokyo 182-0012, Japan
[2)]Graduated School of Science and Technology, Keio University, 3-14-1 Hiyoshi, Kohoku-ku, Yokohama 223-8522, Japan
[3)]Faculty of Science and Technology, Keio University, 3-14-1 Hiyoshi, Kohoku-ku, Yokohama 223-8522, Japan

(Received 25 October 2005; Revised 27 January 2006)

ABSTRACT–For practical application on the HCCI engine, the solution of subjects, such as control of auto-ignition timing and avoidance of knocking, is indispensable. This study focused on the technique of controlling HCCI combustion appropriately, changing the mixture ratio of two kinds of fuel. Methane and DME/*n*-Butane were selected as fuels. The influences, which the mixing ratio of two fuels does to ignition timing, ignition temperature, rate of heat release and oxidation reaction process, were investigated by experiment with 4-stroke HCCI engine and numerical calculation with elementary reactions.

KEY WORDS : Engine, Combustion, Ignition, Knocking, HCCI, Methane, DME, *n*-Butane, Numerical calculation

1. INTRODUCTION

The Homogeneous Charge Compression Ignition (HCCI) engine is a type of engine in which the pre-mixture of fuel and air is introduced into the combustion chamber and is ignited by adiabatic compression of the piston (Thring, 1989; Igarashi and Iida, 2000; Choi *et al.*, 2004). The HCCI engine can be operated under an ultra lean fuel condition and is able to achieve both high efficiency and low emission. However, ignition depends on the ignition temperature of the kind of fuel and in using a single fuel it is difficult to control the ignition timing. The controlling of combustion duration and the evasion of knocking are also problems.

In past studies, the solutions for these problems have been suggested: the method for controlling combustion duration by the introduction of heterogeneity of the fuel concentration in the fuel/air mixture (Kumano and Iida, 2004), the method for controlling ignition timing by mixing a number of hydrocarbons (Shibata *et al.*, 2005; Konno and Chen, 2005; Ogawa *et al.*, 2003) or by using reformed gas such as Hydrogen and Carbon Monoxide as the fuel (Shudo *et al.*, 2003; Sato *et al.*, 2004).

This study focuses on the control method of mixing a number of hydrocarbon fuels similar to the research of Konno and others (Konno and Chen, 2005). The objective of this study is to investigate the effect of the mixing ratio of double componential fuels on HCCI combustion. DME, *n*-Butane and Methane were chosen as the test fuels. At first, the auto-ignition characteristics of each single fuel were investigated. Next, mixing DME or *n*-Butane with Low Temperature Reaction (LTR) and Methane without LTR, the influence of the mixing ratio of these fuels on in-cylinder gas pressure, in-cylinder gas temperature, rate of heat release, ignition timing and ignition temperature were investigated by experiment. Next, the effect of the mixing ratio on oxidation processes was also investigated by using numerical calculations with elementary reactions.

2. TEST FUELS

In this study, DME, *n*-Butane and Methane were used as the test fuels both in the experiment and in the numerical calculations with elementary reactions. The properties of these three fuels were shown in Table 1. DME has the structure with an O atom and the bonding energy of C-H is lower than that of Methane. In addition, the Negative Temperature Coefficient (NTC) region exists due to LTR. *n*-Butane has straight-chain structure and also has LTR in the auto-ignition process. The heat release value due to LTR of *n*-Butane is lower than that of DME. Methane

*Corresponding author. e-mail: su-sato@ntsel.go.jp

with only one carbon atom has the easiest structure of the hydrocarbons. It has only primary C-H bonding and has very high bonding energy. Therefore, the ignition occurs in high temperature and the reaction in low temperature does not appear.

3. RESEARCH METHODS

3.1. Experimental Methods

The specifications of the 4-stroke engine used, appropriate in the experiment are shown in Table 2, and the experimental apparatus in Figure 1. The fuels were continuously injected into the intake manifold about 1500 mm upstream from the intake valve. The fuels were injected in the counter direction to the flow of the intake air in order to form a homogeneous charge. The intake air was introduced into the combustion chamber without heating. The in-cylinder gas pressure was measured with a piezoelectric pressure transducer for all operating conditions. For each test point, the cylinder pressure was sampled over 64 cycles at intervals of 1-degree crank angle.

Table 2. Engine specifications.

	Experiment	Calculation
Process	4-stroke	Only 1 compression and expansion
Displacement	1132 cc	
Bore × Stroke	112 mm × 115 mm	
Length of conrod	250 mm	
Crank radius	57.5 mm	
Intake valve close	ABDC 47°	
Exhaust valve open	BBDC 47°	
Compression ratio	21.6	
Engine speed	960 rpm	

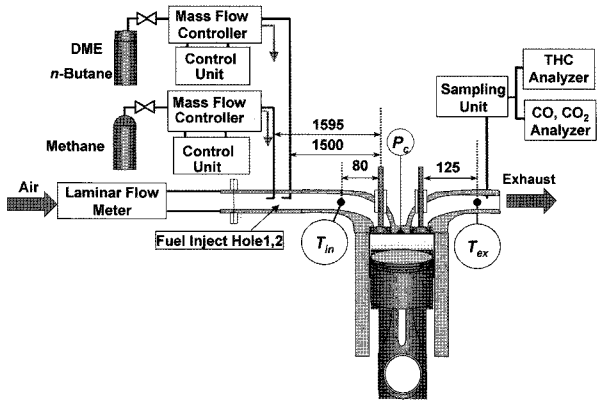

Figure 1. Experimental apparatus.

3.2. Calculation Method of the In-cylinder Gas Temperature in the Experiment

In this experiment, in-cylinder gas temperature was calculated in the following ways. Temperature at the start of compression T_0 (ABDC48°) was calculated by the enthalpy balance Equation (1), using fresh gas temperature T_f, residual gas temperature T_r, mass of fresh gas m_f, mass of residual gas m_r, specific heat at constant pressure of fresh gas c_{p_f} and specific heat at constant pressure of residual gas c_{p_r}. T_f was assumed to be equal to intake air temperature T_{in} and T_r to be equal to exhaust gas temperature T_{ex}. Before the ignition, in-cylinder gas temperature T_c is calculated from Equation (2) assuming adiabatic compression, because the ignition occurs around the center of the combustion chamber, which is not influenced by the heat loss from the cylinder wall. After the ignition, in-cylinder gas temperature is calculated from the ideal gas Equation (3). Adiabatic change is not approved because of heat release.

$$T_0=\frac{m_f \cdot c_{p\_f} \cdot T_f + m_r \cdot c_{p\_r} \cdot T_r}{m_f \cdot c_{p\_f} + m_r \cdot c_{p\_r}} \quad (1)$$

$$T_c(\theta_i)=\left(\frac{P_c(\theta_i)}{P_c(\theta_{i-1})}\right)^{\frac{\kappa-1}{\kappa}} T_c(\theta_{i-1}) \quad (2)$$

$$T_c(\theta_i)=\frac{P_c(\theta_i) \cdot V_c(\theta_i) \cdot n(\theta_{i-1})}{P_c(\theta_{i-1}) \cdot V_c(\theta_{i-1}) \cdot n(\theta_i)} T_c(\theta_{i-1}) \quad (3)$$

Quantifiers;
T : gas temperature [K], m : mass of gas [kg], c_p : specific heat at constant pressure [J/(kg·K)], θ : crank angle [deg], P : gas pressure [MPa], κ : specific heat ratio, V : gas volume [m^3], n : mole number [mol]
Subscripts;
0 : compression start timing, f : fresh gas, r : residual gas, c : in-cylinder gas

Table 1. Test fuel.

Fuel name	Methane	DME	*n*-Butane
Molecular structure		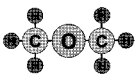	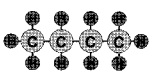
Molecular mass	16.049	46.069	58.12
Low heat release value [MJ/kg]	48.3	28.8	45.6
Cetane number	0	55-60	< 10
Self-ignition temperature [K]	905	623	703
Low temperature reaction	×	O	O

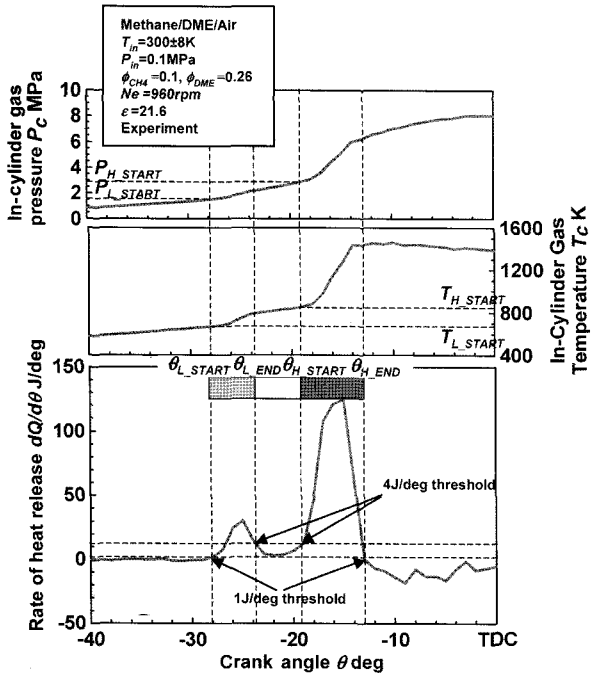

Figure 2. Definition of start and end timings of LTR and HTR.

3.3. The Definition Methods of Start Timing and End Timing of Low Temperature Reaction and High Temperature Reaction

Figure 2 shows the definitions of the start timing and end timing of LTR and High Temperature Reaction (HTR). The start timings and the end timings of both reactions were defined using threshold values for the rate of heat release. That is, the LTR start timing θ_{L_START} was defined as the time when the rate of heat release exceeds 1 J/deg threshold for the first time after compression starts, and the LTR end timing θ_{L_END} was defined as the time when the value drops below 4 J/deg threshold for the first time after the peak timing of the heat release due to LTR. In the case of HTR, its start timing θ_{H_START} was the time when the rate of heat release value exceeds 4 J/deg threshold again after LTR end timing, the end timing θ_{H_END} was the time when the value drops down 1 J/deg threshold after the peak timing of the heat release due to HTR.

3.4. Methods of Numerical Calculation With Elementary Reactions

CHEMKIN II (Kee *et al.*, 1989) and SENKIN (Luz *et al.*, 1988) codes were used to calculate the chemical kinetics of the elementary reactions. These calculations are 0-dimensional. In other words, the calculations were carried out based on the assumption that pressure, temperature and distribution of chemical species are completely uniform. Curran's scheme (species: 78, reactions: 336)

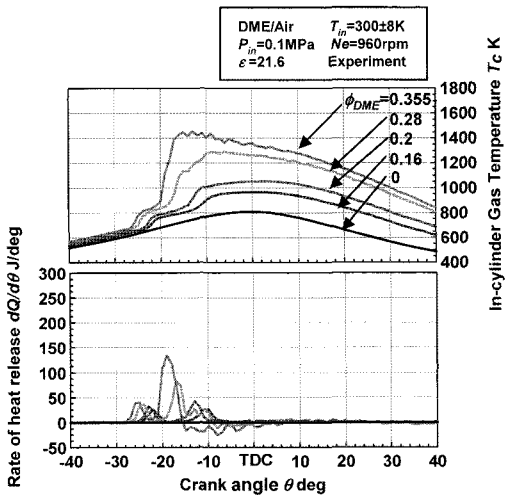

Figure 3. The histories of in-cylinder gas temperature and rate of heat release for various equivalence ratios of DME (experiment).

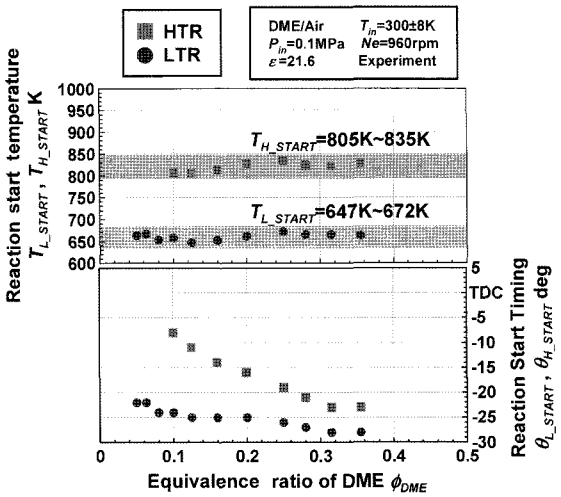

Figure 4. Reaction start timings and temperatures for various equivalence ratios of DME (experiment).

(Curran *et al.*, 1998) was selected as the elementary reaction scheme of Methane and DME, Kojima's scheme (species: 141, reactions: 470) (Kojima, 1994) was selected as that of Methane and *n*-Butane.

4. EXPERIMENTAL RESULTS

4.1. Auto-ignition Characteristics of Single Fuel

First, before the research about double componential fuels, an investigation about the basic characteristics of HCCI combustion for each of the single fuels, which were DME, *n*-Butane and Methane, was carried out. In this experiment, the engine speed *Ne* was set at 960 rpm (16 Hz), the compression ratio *e* at 21.6, the intake air

temperature at T_{in}=300±8 K and the intake air pressure at P_{in}=0.1 MPa. The experimental parameter was the equivalence ratio ϕ of each fuel.

4.1.1. Auto-ignition characteristics of DME

Figure 3 shows the histories of in-cylinder gas pressure, in-cylinder gas temperature and rate of heat release for various equivalence ratios of DME. At ϕ_{DME}=0.16, there are two rises of pressure and temperature and two stages of heat release. The first stage was due to LTR and the second one was due to HTR. With the increase in equivalence ratio, the start timing of LTR and HTR advanced, the maximum values of pressure and temperature rose and the peak value of heat release due to LTR and HTR increased. At ϕ_{DME}=0.355, a vibration due to knocking was observed, and in an equivalence ratio that was higher than 0.355, engine operation became impossible because of knocking. The reaction start timings and the reaction start temperatures are shown in Figure 4. The circle indicates LTR start and the square indicates HTR start. The start timings of LTR and HTR advanced with the increase of the equivalence ratio of DME. However, the start temperatures of LTR were within the range from 647 K to 672 K, and those of HTR were within the range from 805 K to 835 K.

4.1.2. Auto-ignition characteristics of *n*-Butane

Figure 5 shows the histories of in-cylinder gas temperature and rate of heat release for various equivalence ratios of *n*-Butane. With the increase in equivalence ratio, the start timing of HTR advanced, the maximum value of temperature rose and the peak value of heat release due to LTR and HTR increased. These phenomena were the same as in the DME case. However, heat release due to

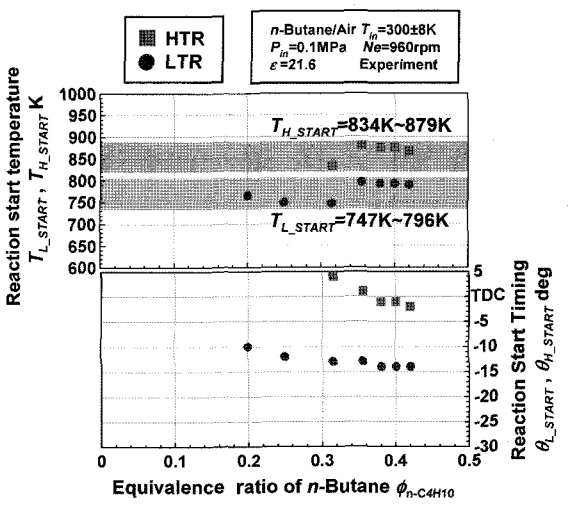

Figure 6. Reaction start timings and temperatures for various equivalance ratios of *n*-Butane (experiment).

LTR was much less than for DME. The reaction start timings and the reaction start temperatures are shown in Figure 6. The start timings of LTR and HTR advanced with the increase of the equivalence ratio of *n*-Butane. However, the start temperatures of LTR were within the range from 747 K to 796 K, and those of HTR were within the range from 834 K to 879 K.

4.1.3. Auto-ignition characteristics of methane

The histories of in-cylinder gas temperature and rate of heat release of Methane/air pre-mixture are shown in Figure 7. In this figure, the dotted line indicates the history under the same conditions as Figure 3 and Figure 4, which were natural aspiration and no heating of intake

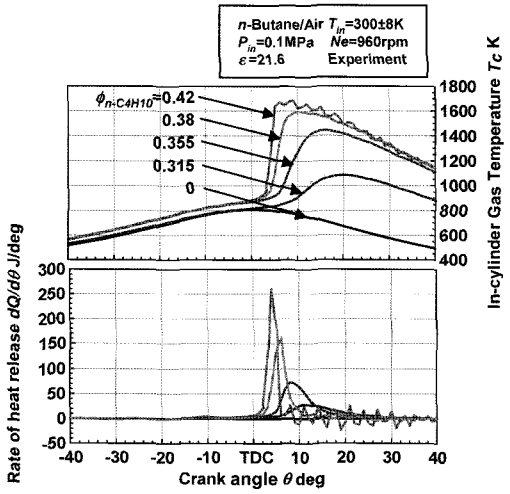

Figure 5. The histories of in-cylinder gas temperature and rate of heat release for various equivalence ratios of *n*-Butane (experiment).

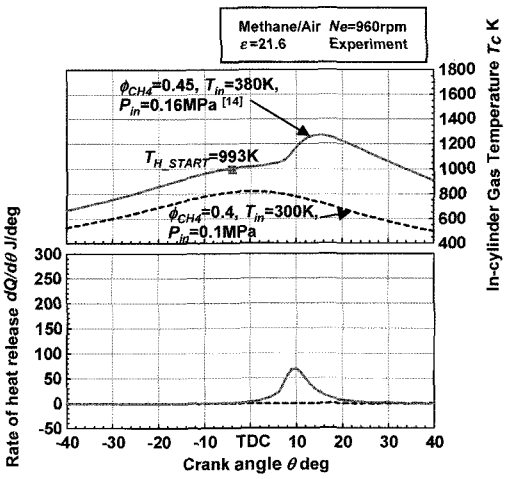

Figure 7. The histories of in-cylinder gas temperature and rate of heat release and reaction start temperature of Methane/air mixture (experiment).

air. Under these conditions, ignition did not occur. In order to confirm the ignition temperature of Methane, other data for the experiment conducted by Keio University was refered to (Jun *et al.*, 2003). In Figure 7, the solid line shows the histories for Methane when the equivalence ratio is ϕ_{CH4}=0.45, with the intake air heated and supercharged. Because of heating and supercharging, the ignition timing cannot be referred. The start temperature of HTR of Methane was 993 K.

4.2. Operating Regions of HCCI Combustion When Double Componential Fuels are Used

The combustion experiment using mixed fuel of Methane and DME was carried out by varying the Methane-based equivalence ratio ϕ_{CH4}, and the DME-based equivalence ratio ϕ_{DME}. In this experiment, the engine speed *Ne* was set at 960 rpm (16 Hz), the compression ratio *e* at 21.6, the intake air temperature at T_{in}=300±8 K and the intake air pressure at P_{in}=0.1 MPa. In Figure 8, all of the experiment points and operating region are shown. "x" indicates a misfiring point, "●" indicates the point that was able to realize HCCI combustion and "▲" indicates a knocking point. The variation of DME-based equivalence ratio on the vertical axis shows the variation of Figure 3. When ϕ_{DME} increased, the equivalence ratio of the knock limit was low. On the contrary, when ϕ_{CH4} increased, the equivalence ratio region limited by knocking was expanded. Especially at ϕ_{DME}=0.1, the region which the engine can be operated was expanded to ϕ_{CH4}=0.5 (total equivalence ratio ϕ_{total}=0.6).

Next, under the same conditions as the Methane/DME case, the experiment was carried out by varying the Methane-based equivalence ratio ϕ_{CH4}, and the *n*-Butane-based equivalence ratio $\phi_{n\text{-}C4H10}$. The map of operating region was shown in Figure 9. The meaning that the sign shows is the same as Figure 8. The variation of *n*-Butane-based equivalence ratio on the vertical axis shows the variation of Figure 5. When ϕ_{total} was increased only by *n*-Butane, knocking occurred at $\phi_{n\text{-}C4H10}$=0.42. At $\phi_{n\text{-}C4H10}$=0.4, the region which the engine can be operated was expanded to ϕ_{CH4}=0.2 (total equivalence ratio ϕ_{total} =0.6). Comparing with Figure 8, though the region is different, almost the same heat quantity can be input into the engines.

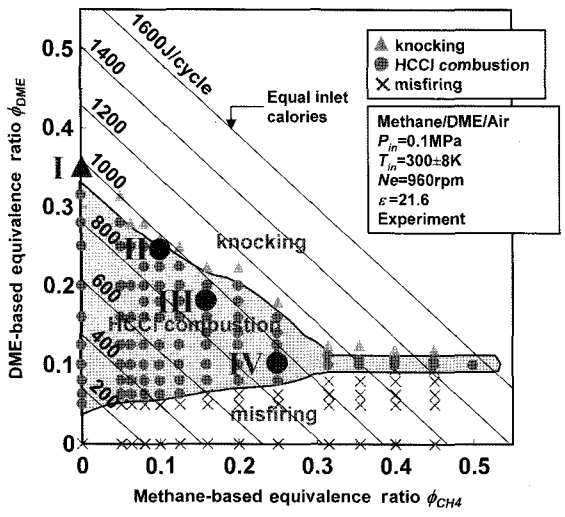

Figure 8. Map of operating region in the experiment of Methane/DME/air mixture (experiment).

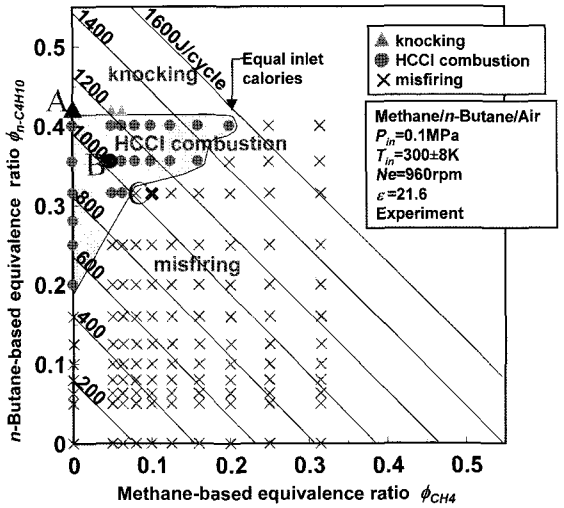

Figure 9. Map of operating region in the experiment of Methane/*n*-Butane/air mixture (experiment).

4.3. The Effect of the Mixing Ratio of Double Componential Fuels on HCCI Combustion Process

In HCCI combustion using single fuel, when the total equivalence ratio increases, HCCI ignition is advanced (Igarashi and Iida, 2000). In this section, under the conditions that the inlet heat quantity is constant, it analyzed about the case where the mixing ratio of Methane and DME or Methane and *n*-Butane changes. The points of I, II, III and IV in Figure 8 and A, B and C in Figure 9 were picked up. In addition, the influence of mixing ratio of double componential fuels on ignition timing and ignition temperature was considered.

4.3.1. Effect of the mixing ratio of methane/DME

Figure 10 shows the histories of in-cylinder gas pressure, in-cylinder gas temperature and the rate of heat release, and combustion duration in varying Methane-based equivalence ratio and DME-based equivalence ratio for I: ϕ_{CH4}=0, ϕ_{DME}=0.355, II: 0.1, 0.25, III: 0.16, 0.18 and IV: 0.25, 0.1, under the condition of constant inlet heat quantity of Q_{in}=960±25J. When the fuel is only DME (condition I), the first pressure rise was observed at

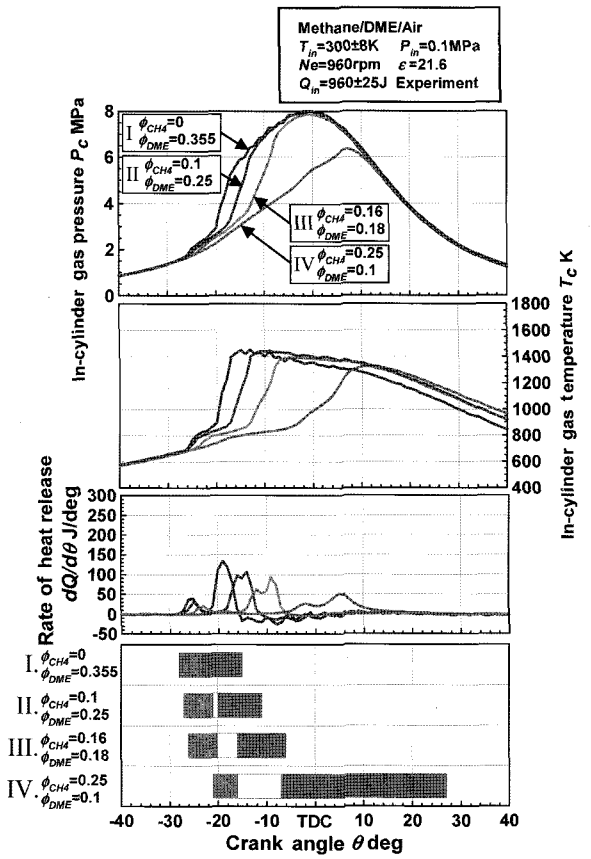

Figure 10. Histories of in-cylinder gas pressure, in-cylinder gas temperature and rate of heat release, and combustion duration for various mixing ratios of Methane and DME (experiment).

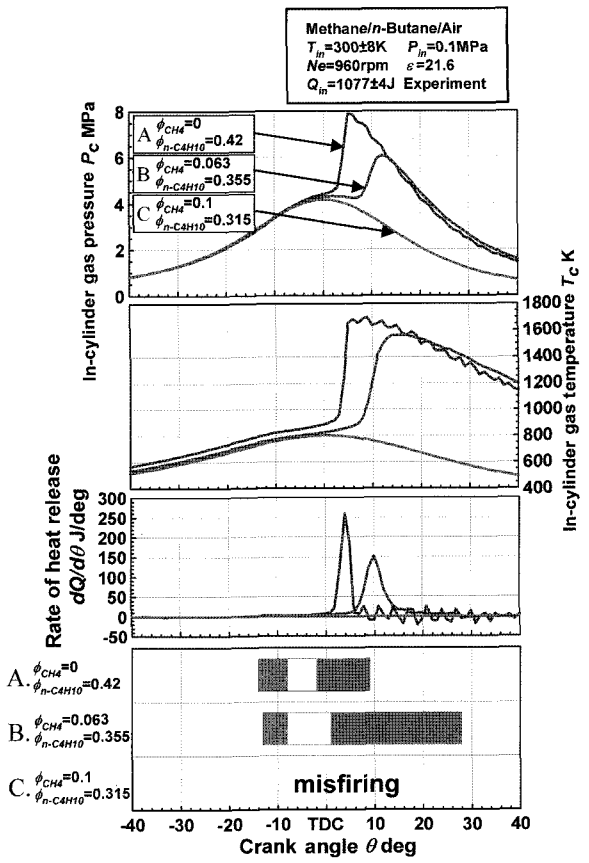

Figure 11. Histories of in-cylinder gas pressure, in-cylinder gas temperature and rate of heat release, and combustion duration for various mixing ratios of Methane and *n*-Butane (experiment).

BTDC28° and the second one was observed at BTDC23°. In the condition I, a vibration of pressure history caused by knocking was observed. Both of the LTR start timing and the HTR start timing were retarded as the increase of the ratio of Methane. Furthermore, the decrease of heat release quantity due to LTR, the division of HTR to two stages and the reduction of the maximum value of HTR were observed. Especially, in the condition IV, the maximum value was decreased to about 50J/deg, and the peak timing of the heat release of HTR was ATDC5°. For combustion duration, with the increase of the ratio of Methane, the duration of degeneration and HTR duration were lengthened. From these results, it was shown by adjustment of the mixing ratio of Methane and DME that it is possible to control ignition timing and heat release generating timing, even if the inlet heat quantity was constant.

4.3.2. Effect of the mixing ratio of methane/*n*-Butane

Figure 11 shows the histories of in-cylinder gas pressure, in-cylinder gas temperature and the rate of heat release, and combustion duration in varying Methane-based equivalence ratio and *n*-Butane-based equivalence ratio for A: ϕ_{CH4}=0, $\phi_{n\text{-}C4H10}$=0.42, B: 0.063, 0.355, C: 0.1, 0.315, under the condition of constant inlet heat quantity of Q_{in}=1077±4J. When the fuel is only *n*-Butane (condition A), the pressure rise and the temperature rise were observed at around TDC. In the condition B, the timings of these rise points were retarded by increase of the ratio of Methane. In the condition C, ignition did not occur. Comparing with the history of heat release of A and that of B, although little heat release due to LTR were observed, the heat release timing of HTR of B was retarded and the maximum value of the heat release was decreased from 260J/deg to 150J/deg. According to the definition method of ignition timing, the duration of LTR could be defined. The start timings of LTR and HTR were retarded and the duration of HTR was lengthened to 27°. The results that the decrease of the maximum value of heat release and the lengthening of the duration due to HTR with the increase of the ratio of Methane were the

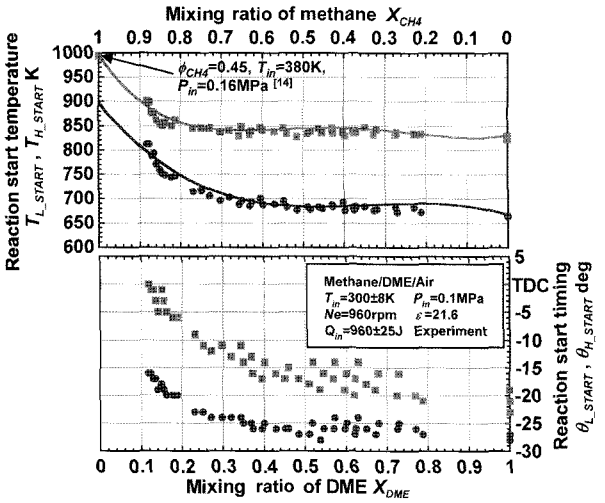

Figure 12. Effect of the mixing ratios of DME and Methane on reaction start timings and temperatures (experiment).

same as the case of Methane/DME.

4.3.3. The Effect of the mixing ratio of the double componential fuels on ignition timing and ignition temperature

Figure 12 shows the reaction start timings and the reaction start temperatures for the case of Methane/DME/air mixture, and all points in this figure are the points at which the combustion efficiencies are over 50%. X_{DME} means the mixing mol ratio of DME. With the increase of DME ratio, the reaction start timings of LTR and HTR advanced and reaction start temperatures became lower. Though these points include various inlet heat quantity

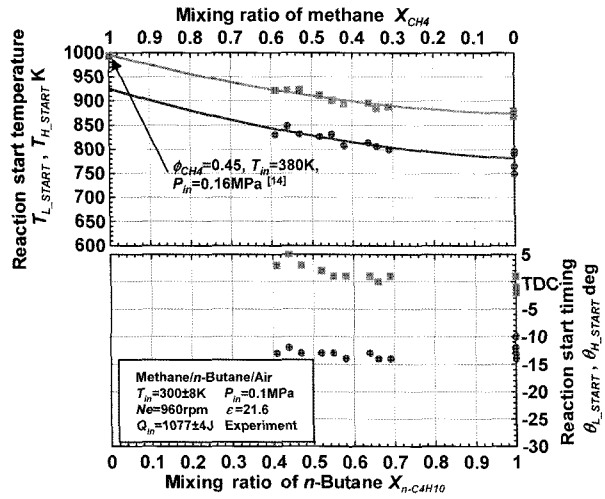

Figure 13. Effect of the mixing ratios of n-Butane and Methane on reaction start timings and temperatures (experiment).

conditions, it is possible to express the start temperatures of LTR and HTR as functions of the mixing ratio of DME.

Figure 13 shows the relationship between the mixing ratio of n-Butane and the reaction start timings and the reaction start temperatures. For the start temperatures of LTR and HTR, the difference in the range of start temperatures was smaller than in the case of Methane/DME/air. However, it is also possible to express the start temperatures of LTR and HTR as functions of the mixing ratio of n-Butane regardless of inlet heat quantity.

5. CALCULATION RESULTS

From the experimental results described above, it is clarified that the increase of the ratio of Methane retarded

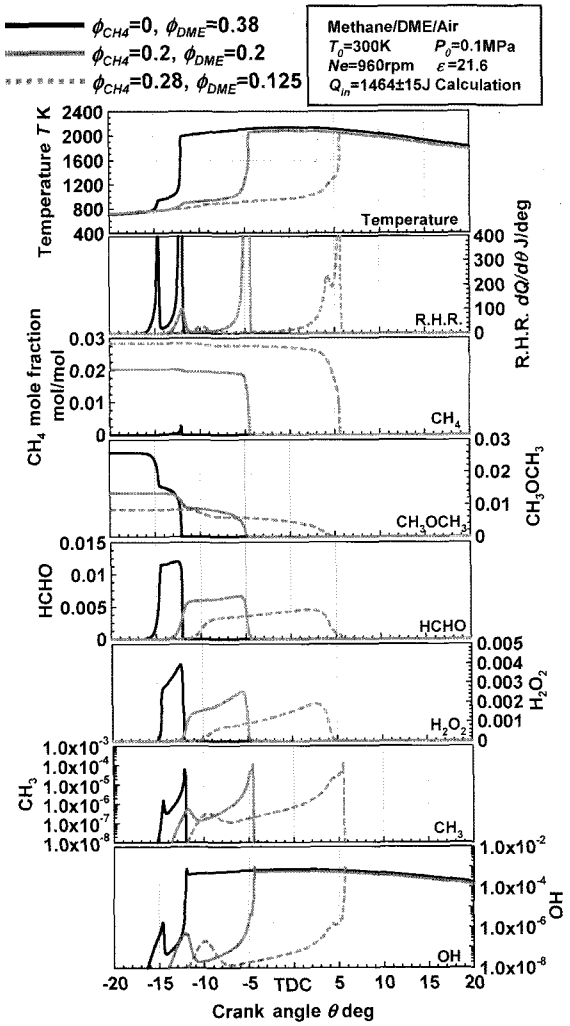

Figure 14. Histories of temperature, the rate of heat release and mole fractions of Methane, DME, HCHO, H_2O_2, CH_3 and OH for various mixing ratios of Methane and DME (calculation).

ignition timing and suppress the maximum value of the rate of heat release both in cases of Methane/DME and Methane/*n*-Butane. In order to look into how the chemical reactions occur, the investigation by numerical calculation with elementary reactions was performed.

5.1. Reaction Process of Methane/DME/air Mixture

The calculations were carried out in varying the mixing ratios of Methane and DME, under the conditions of T_0=300 K, P_0=0.1 MPa, *Ne*=960 rpm, ε=21.6 and Q_{in}= 1464±15J. Figure 14 shows the temperature histories, the histories of the rate of heat release and mole fraction histories of Methane, DME, HCHO, H_2O_2, CH_3 and OH at the three conditions of [ϕ_{CH4}=0, ϕ_{DME}=0.38], [ϕ_{CH4}=0.2, ϕ_{DME}=0.2], [ϕ_{CH4}=0.28, ϕ_{DME}=0.125]. In any condition, LTR and HTR occurred and generation of HCHO, H_2O_2, CH_3 and OH in LTR was observed. When including Methane in the fuel, Methane was slightly oxidized at LTR. This is why OH radicals, which were generated from HCHO and H_2O_2 at LTR, had the effect to oxidize Methane. HTR was separated into two stages, and at the first stage of HTR Methane was rapidly oxidized and CH_3 increased at the same time. Mixing Methane and DME, OH radicals made from intermediate products accelerate the oxidation of Methane at LTR duration and at the first stage of HTR. As a result, the heat release at the final stage of HTR was weakened and rapid combustion reaction was suppressed.

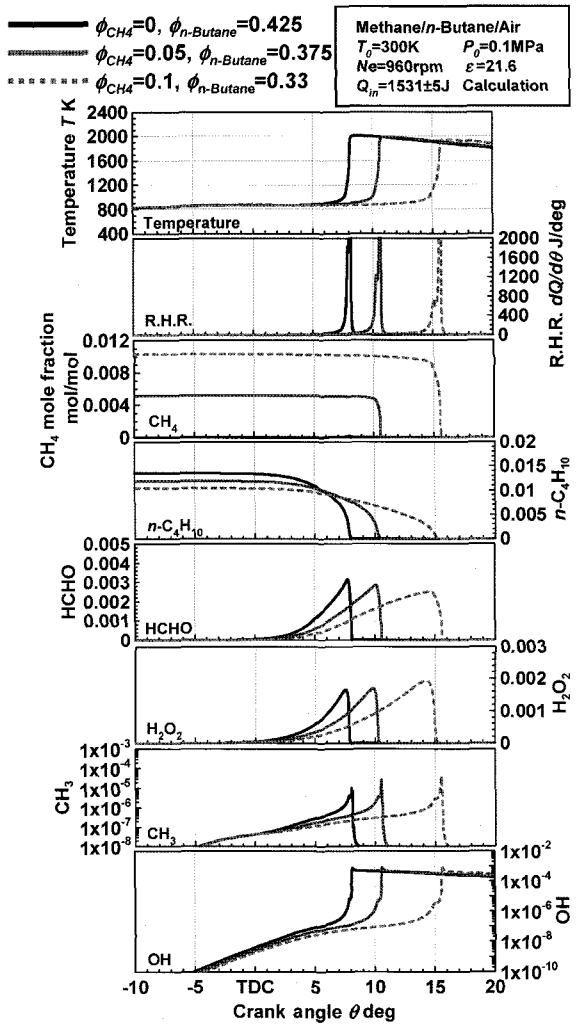

Figure 15. Histories of temperature, the rate of heat release and mole fractions of Methane, *n*-Butane, HCHO, H_2O_2, CH_3 and OH for various mixing ratios of Methane and *n*-Butane (calculation).

5.2. Reaction Process of Methane/*n*-Butane/air Mixture

The calculations were carried out in varying the mixing ratios of Methane and *n*-Butane, under the conditions of T_0=300 K, P_0=0.1 Mpa, *Ne*=960 rpm, ε=21.6 and Q_{in}= 1531±5J. Figure 15 shows the temperature histories, the histories of the rate of heat release and mole fraction histories of Methane, *n*-Butane, HCHO, H_2O_2, CH_3 and OH at the three conditions of [ϕ_{CH4}=0, $\phi_{n\text{-}C4H10}$=0.425], [ϕ_{CH4}=0.05, $\phi_{n\text{-}C4H10}$=0.375], [ϕ_{CH4}=0.1, $\phi_{n\text{-}C4H10}$=0.33]. The timing when Methane was rapidly oxidized was the first stage of HTR in same manner as Figure 10. In any condition, LTR did not occur and the amounts of HCHO, H_2O_2 generated until HTR start were small. As a result, the supply timing of OH radicals effecting oxidation of Methane was later than the case of Methane/DME.

6. CONCLUSIONS

The objective of this study is to investigate the effect of the mixing ratio of double componential fuels on HCCI combustion. By mixing Methane and DME or *n*-Butane, the influence of the mixing ratio of these fuels on in-cylinder gas pressure, in-cylinder gas temperature, rate of heat release, ignition timing and ignition temperature was experimentally investigated. Next, the effect of the mixing ratio on oxidation processes was also investigated by using numerical calculations with elementary reactions. The following knowledge was acquired as the result of investigation.

As a result of experimenting with the single fuel; in the case of DME, the start temperatures of HTR were within the range from 805 K to 835 K and in the case of *n*-Butane were within the range from 834 K to 879 K, regardless of equivalence ratio.

As a result of experimenting, in both the Methane/DME case and the Methane/*n*-Butane case, the engine could operate at the total equivalence ratioof 0.6 at the maximum. The operating region was different in these two cases.

In both Methane/DME case and the Methane/*n*-Butane case, when the mixing ratios of the two fuels were

changed, with the increase of Methane the start timing of HTR was retarded, the duration of HTR was lengthened and the maximum value of the rate of heat release decreased.

When mixing Methane and DME, LTR appearance temperature and HTR appearance temperature became higher with the increase of Methane. On the other hand, when mixing Methane and *n*-Butane, HTR appearance temperature became lower with the increase of Methane. In all cases, the increase of Methane enables retardation of ignition timing and the suppression of the rate of heat release.

As a result of experimenting with the double componential fuel, in both cases of Methane/DME and Methane/*n*-Butane, it is possible to express the start temperatures of LTR and HTR as functions of the mixing ratios of the double componential fuels, regardless of inlet heat quantity.

When mixing Methane and DME, OH radicals made from HCHO and H_2O_2 accelerate the oxidation of Methane at even LTR duration. As a result, heat release at HTR was suppressed. On the other hand, when mixing Methane and *n*-Butane, reactions at LTR were weak and the effect of OH radicals on Methane oxidation did not appear until HTR.

REFERENCES

Choi, G. H., Han, S. B. and Dibble, R. W. (2004). Experimental study on homogeneous charge compression ignition egine operation with exhaust gas recirculation. *Int. J. Automotive Technology* **5, 3,** 195–200.

Curran, H. J., Pitz, W. J., Westbrook, C. K., Dagaut, P., Boettner, J-C. and Cathonnet, M. (1998). A wide range modeling study of dimethyl ether oxidation. *Int. J. Chemical Kinetics* **30, 3**, 229–241.

Igarashi, T. and Iida, N. (2000). Auto ignition and combustion of DME and *n*-Butane/Air mixtures in homogeneous charge compression ignition engine. *SAE Paper No.* 2000-01-1832.

Jun, D., Ishii, K. and Iida, N. (2003). Combustion analysis of natural gas in a four stroke HCCI engine using experiment and elementary reactions calculation. *SAE Paper No.* 2003-01-1089.

Kee, R. J., Rupley, F. M. and Miller, J. A. (1989). *CHEMKIN-II: A FORTRAN Chemical Kinetics Package for the Analysis of Gas-Phase Chemical Kinetics.* Sandia National Laboratories Report. SAND89-8009B.

Kojima, S. (1994). Detailed modeling of *n*-Butane autoignition chemistry. *Combustion and Flame*, **99**, 87–136.

Konno, M. and Chen, Z. (2005). Ignition mechanisms of HCCI combustion process fueled with methane/DME composite fuel. *SAE Paper No.* 2005-01-0182.

Kumano, K. and Iida, N. (2004). Analysis of the effect of charge inhomogeneity on HCCI combustion by chemiluminescence measurement. *SAE Paper No.* 2004-01-1902.

Luz, A. E., Kee, R. J. and Miller, J. A. (1988). *SENKIN: A FORTRAN Program for Predicting Homogeneous Gas Phase Chemical Kinetics with Sensitivity Analysis.* Sandia National Laboratories Report. SAND87-8248.

Ogawa, H., Miyamoto, N., Kaneko, N. and Ando, H. (2003). Combustion control and operating range expansion with direct injection of reaction suppressors in a premixed DME HCCI engine. *SAE Paper No.* 2003-01-0746.

Sato, S., Yamasaki, Y., Kawamura, H. and Iida, N. (2004). Research on the influence on natural gas HCCI combustion of hydrogen and carbon monoxide. *COMODIA 2004*, 247–254.

Shibata, G., Oyama, K., Urushihara, T. and Nakano, T. (2005). Correlation of low temperature heat release with fuel composition and HCCI engine combustion. *SAE Paper No.* 2005-01-0138.

Shudo, T., Ono, Y. and Takahashi, T. (2003). Ignition control by DME-Reformed gas in HCCI combustion of DME. *SAE Paper No.* 2003-01-1824.

Thring, R. H. (1989). Homogeneous-charge compression-ignition (HCCI) engine. *SAE Paper No.* 892068.